JOURNAL OF THE ROYAL SOCIETY Interface

Physical methods for investigating structural colours in biological systems

P Vukusic and D.G Stavenga

J. R. Soc. Interface 2009 **6**, S133-S148 first published online 21 January 2009
doi: 10.1098/rsif.2008.0386.focus

Interface focus

J. R. Soc. Interface (2009) **6**, S133–S148
doi:10.1098/rsif.2008.0386.focus
Published online 21 January 2009

Physical methods for investigating structural colours in biological systems

P. Vukusic[1,*] and D. G. Stavenga[2]

[1]*School of Physics, University of Exeter, Exeter EX4 4QL, UK*
[2]*Department of Neurobiophysics, University of Groningen, Nijenborgh 4, 9747 AG Groningen, The Netherlands*

Many biological systems are known to use structural colour effects to generate aspects of their appearance and visibility. The study of these phenomena has informed an eclectic group of fields ranging, for example, from evolutionary processes in behavioural biology to micro-optical devices in technologically engineered systems. However, biological photonic systems are invariably structurally and often compositionally more elaborate than most synthetically fabricated photonic systems. For this reason, an appropriate gamut of physical methods and investigative techniques must be applied correctly so that the systems' photonic behaviour may be appropriately understood. Here, we survey a broad range of the most commonly implemented, successfully used and recently innovated physical methods. We discuss the costs and benefits of various spectrometric methods and instruments, namely scatterometers, microspectrophotometers, fibre-optic-connected photodiode array spectrometers and integrating spheres. We then discuss the role of the materials' refractive index and several of the more commonly used theoretical approaches. Finally, we describe the recent developments in the research field of photonic crystals and the implications for the further study of structural coloration in animals.

Keywords: structural colour; photonics; iridescence; multilayers; spectrometry; microscopy

1. INTRODUCTION

The visual appearances of biological systems have been investigated and characterized using numerous different methods. The results, invariably collected using a range of microscopic, optical interrogation and modelling techniques, have been wide reaching. They have offered insight into a variety of biological topics such as: species' behaviour and communication; crypsis strategies and pressure-driven adaptation methods; and morphological, developmental and evolutionary processes (e.g. Fox & Vevers 1960; Silberglied & Taylor 1973; Durrer 1977; Prum 2006). Furthermore, many of the investigations have revealed ingenious optical and photonic system designs that are appropriate for biomimetic synthetic replication (Forbes 2006).

Particular recent advances have been made in the study and understanding of animals that exhibit structural colour. Structural colour comprises the optical effects produced when incident electromagnetic radiation (such as visible, ultraviolet and near-infrared light) encounters ordered spatial variations in a sample's constituent dielectric material that are on the same length scale as the wavelength of the incident light. A dielectric material is characterized by its refractive index (RI); its value only has a real component when it comprises no optical absorption, and it has both real and imaginary components when light is absorbed. The spatial distribution of the sample's constituent dielectric material, and hence its RI, will largely determine the flow of light through or from it. It is this light scattering, in reflection and transmission, which subsequently determines the object's visual appearance.

It is now well known that, generally, biological objects with inhomogeneous irregular RI distributions are colourless or diffusely white when there is no absorption. However, when their constituent RI distributions have ordered or quasi-ordered sub-micrometre domains, then wavelength-dependent coherent scattering can occur. This can give rise to bright structural colours (Mason 1926, 1927; Ghiradella *et al.* 1972; Schultz & Rankin 1985; Vukusic *et al.* 2000, 2001; Vukusic & Sambles 2003; Kinoshita & Yoshioka 2005; Prum 2006; Kinoshita *et al.* 2008).

The requisite ordered or quasi-ordered variation in the RI for the production of structural colour effects may occur in one, two or three spatial dimensions. Generally, one-dimensional RI modulations create multilayers or surface monogratings; RI variations in two dimensions form analogues of photonic crystal fibres or surface bigratings; and three-dimensional spatial RI modulations are designated as full photonic crystals. In some animals, such as hummingbirds,

*Author for correspondence (p.vukusic@ex.ac.uk).

One contribution of 13 to a Theme Supplement 'Iridescence: more than meets the eye'.

Received 28 October 2008
Accepted 8 December 2008

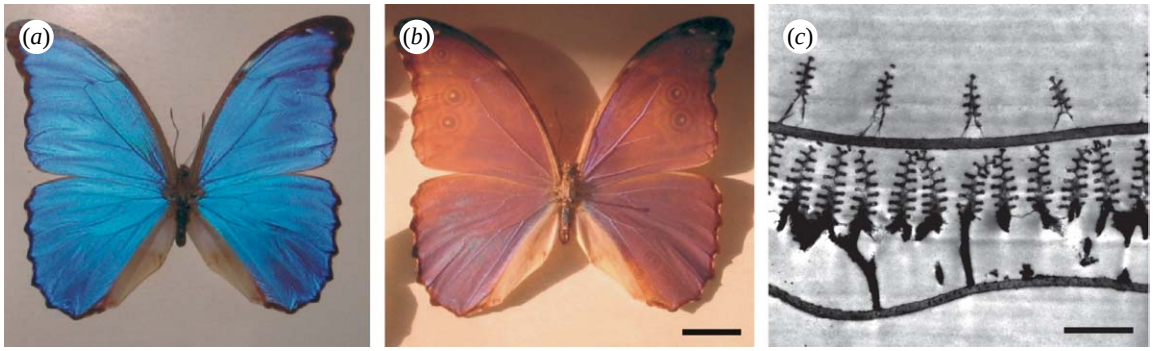

Figure 1. (*a*) The upper wings of the tropical butterfly *M. didius* have a striking blue colour owing to multilayer interference reflection. (*b*) Upon oblique illumination, outside the angle of interference reflection, a light brown pigmentary colour in the wing scales becomes visible. Note the appearance of 'eyespots' from the wings' ventral surfaces, which are often quite marked in the dorsal wings of other butterflies. With wide-angle illumination, the eyespots are completely unnoticed owing to the high intensity of the blue interference reflection. (*c*) TEM image of a cross section through the bilayer of the dorsal wing scales on *M. didius*, showing the highly reflective scale present basally, which is covered by the highly diffractive scale present superficially (Vukusic *et al.* 1999). Scale bars: (*a*,*b*) 1 cm and (*c*) 1.5 μm.

Morpho butterflies and jewel beetles, the systems creating structural colours dominate the animals' visual appearances. In many other examples, however, for instance in male pigeons, brimstone butterflies and tiger beetles, the animals' structural colours may be convolved with one or more pigments, which contribute additional colour or related optical effects due to local and spectrally selective light absorption (Mason 1926, 1927; Vukusic *et al.* 2004; Hariyama *et al.* 2005; Stavenga *et al.* 2006*a*; Yoshioka & Kinoshita 2006*a*; Morehouse *et al.* 2007).

A striking example is one of the icons of structural coloration, the *Morpho* butterfly family. In *Morpho didius* (figure 1), for instance, the dorsal (upper) wing surfaces display a brilliant blue reflection when illuminated from directly overhead (figure 1*a*). This colour effect vanishes upon oblique illumination. Phenomena such as these are controlled by the scales that imbricate *Morpho* wings, as occurs in virtually all lepidoptera. In *M. didius* and other brightly coloured *Morphos*, multilayered structures in the scale ridges reflect blue light that can be strongly dependent on the angle of illumination (Ghiradella 1998; Vukusic *et al.* 1999; Kinoshita *et al.* 2002; Vukusic & Sambles 2003; Kinoshita *et al.* 2008). For instance, with oblique illumination, the dorsal wing scales become largely transparent, and then the more heavily pigmented scales on the ventral (lower) side of the wings become visible (figure 1*b*).

Structurally coloured objects are often iridescent; that is, their colours appear to change with the angle of light incidence (figure 2) or with the observer's perspective. Depending on animal species, this may have a functional role in, for instance, intraspecific communication. Therefore, one of the typical aims of investigating structurally coloured biological systems that exhibit this form of effect would be to develop an understanding of the animal's angle-dependent spectral phenomena from the perspective of their anatomical structure and their constituent material. The chemical properties and associated characterization methods of the materials comprising structurally coloured biological systems are summarized elsewhere (Shawkey *et al.* 2009).

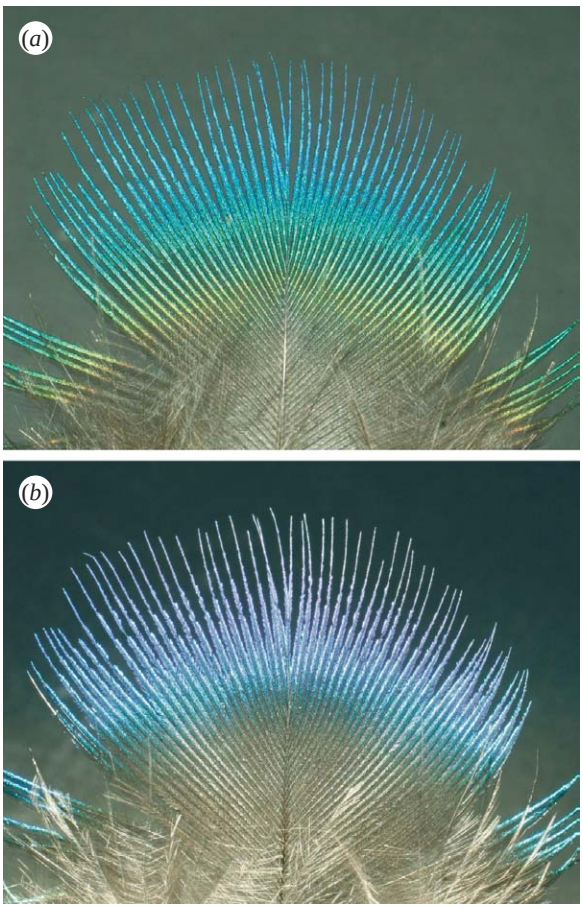

Figure 2. Iridescent feather of a peacock, illuminated from directions differing by approximately 90°.

In all biological systems, it is a complex set of variables that controls or contributes to a specific optical signature and the resulting overall visual appearance. To understand the significance of each of these variables both qualitatively and quantitatively, and to appreciate the way in which they create an animal's complete colour appearance, it is essential to measure the spectral and spatial characteristics of the animal's body reflectance. It is with this in mind that we therefore first introduce the central concept of the

bidirectional reflectance distribution function (BRDF). We subsequently apply this to the experimental methods that are available, and that have been successfully used for investigating structural colours in biological systems. We aim to assess the reliability and the nature of the information to which each method may lead.

2. THE BIDIRECTIONAL REFLECTANCE DISTRIBUTION FUNCTION

From a measurement perspective, biological structural colour effects can have a very broad set of associated experimental variables. These are related to four aspects: the illumination conditions; the measurement or light detection conditions; the structural geometry of the sample; and, lastly, the compositional materials of the sample. Formally, the relation that connects all of these is the BRDF (dimension sr^{-1}; Nicodemus 1965; Nicodemus *et al.* 1977), which is defined as the ratio between the reflected radiance (dimension $\mathrm{W\,m^{-2}\,sr^{-1}}$) and the incident irradiance (dimension $\mathrm{W\,m^{-2}}$; figure 3),

$$R_\lambda(\theta_\mathrm{i},\varphi_\mathrm{i},\theta_\mathrm{r},\varphi_\mathrm{r}) = \frac{I_\mathrm{r}(\theta_\mathrm{r},\varphi_\mathrm{r})\mathrm{d}\omega_\mathrm{r}}{I_\mathrm{i}(\theta_\mathrm{i},\varphi_\mathrm{i})\cos\theta_\mathrm{i}\mathrm{d}\omega_\mathrm{i}}. \qquad (2.1)$$

The BRDF assumes light scattering from only one surface point. This, however, may not always be valid for many macroscopic objects where substantial subsurface scattering occurs. The more general function that incorporates non-negligible subsurface scattering is the bidirectional scattering surface reflectance distribution function (Marschner *et al.* 2001). It is the function that completely describes the interaction of the incident light with a material. For most structurally coloured biological systems, however, strong subsurface scattering (i.e. associated with light that enters the material at one location and emerges at a spatially significantly different location) is negligible, and the limiting case of the more straightforward BRDF is therefore fully adequate (Shimada & Kawaguchi 2005). It should be noted from equation (2.1) that a single BRDF only applies for elastic scattering at a specific wavelength (i.e. fluorescence is negligible). The formal BRDF characterization of a sample, therefore, requires a separate BRDF at each wavelength of interest.

Generally, biological systems are extended objects with large-area surfaces. Accordingly, the task of characterizing a biological sample's visual appearance via its BRDF, both across the entirety of its surface and at all wavelengths of interest, is an extremely challenging undertaking. Measurement of the BRDF even at a single location of, say, a *Morpho* butterfly (figure 1) or a peacock feather (figure 2) is extremely burdensome if it is done via sampling the light scattered into numerous directions $(\theta_\mathrm{r},\varphi_\mathrm{r})$ of the hemisphere above the surface both at each angle of incidence $(\theta_\mathrm{i},\varphi_\mathrm{i})$ in the hemisphere and at different incident wavelengths (figure 3). Realistically, therefore, to provide experimental insight into the scattering processes of a sample, experimental approaches must be appropriately simplified while still generating useful information about the sample's visual appearance. The principal purpose of this paper is to elucidate the ranges of experimental methods that have been successfully used, and which have recently been developed, for investigating structural colours in biological systems.

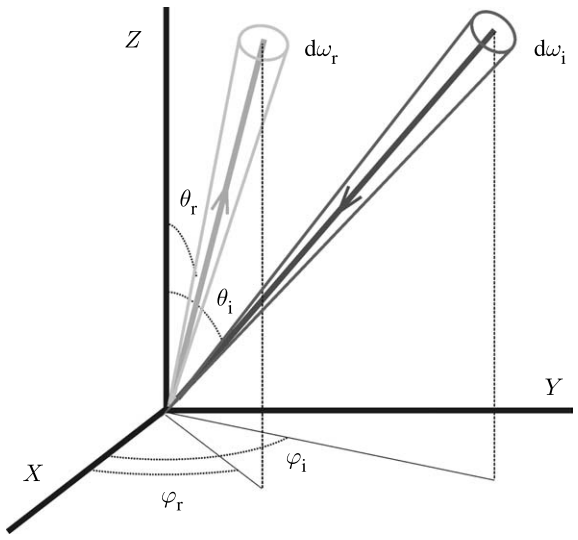

Figure 3. The BRDF relates the reflected light $I_\mathrm{r}(\theta_\mathrm{r},\varphi_\mathrm{r})$ in a small solid angle $\mathrm{d}\omega_\mathrm{r}$ to the incident light flux $I_\mathrm{i}(\theta_\mathrm{i},\varphi_\mathrm{i})$ in a small solid angle $\mathrm{d}\omega_\mathrm{i}$ (see equation (2.1)).

3. MEASURING STRUCTURAL COLORATION

3.1. Spatial spectrophotometry and scatterometry

A straightforward and direct method for measuring light scattering from biological samples is schematically represented in figure 4*a*. It is a method that has been widely used for samples of various sizes from a range of different animals (for a review, see Kinoshita *et al.* 2008). Light from an appropriate narrow or broadband source is focused onto a sample from which it is subsequently scattered. The spatial distribution of this scattered light (both in the reflection and transmission hemispheres) can then be investigated by its collection using a spatially filtered detector or light guide designed to rotate around the sample and deliver it to a spectrometer. Absolute reflectance and transmittance measurements, using a range of monochromatic laser light sources, have been performed on single *Morpho* butterfly scales (Vukusic *et al.* 1999) and single pierid butterfly scales (Morehouse *et al.* 2007). Other detailed spectral analyses were performed on isolated scales of various butterflies (Yoshioka & Kinoshita 2006*b*; Giraldo *et al.* 2008), using a white light source and a diode array spectrometer.

By rotation of the specimen, the BRDF can be measured as a function of the angle of illumination. Alternatively, the light source of figure 4*a* can be replaced by a flexible light guide fitted with a suitable lens, which is rotated around the sample. Spectrophotometry can then be carried out with an experimental arrangement similar to that of figure 4*a* on areas minimally of a few millimetres in diameter (Rutowski *et al.* 2007).

An elegant and effective method for visualizing the spatial light scattering by a small- to medium-sized object, such as a butterfly scale or a bird feather

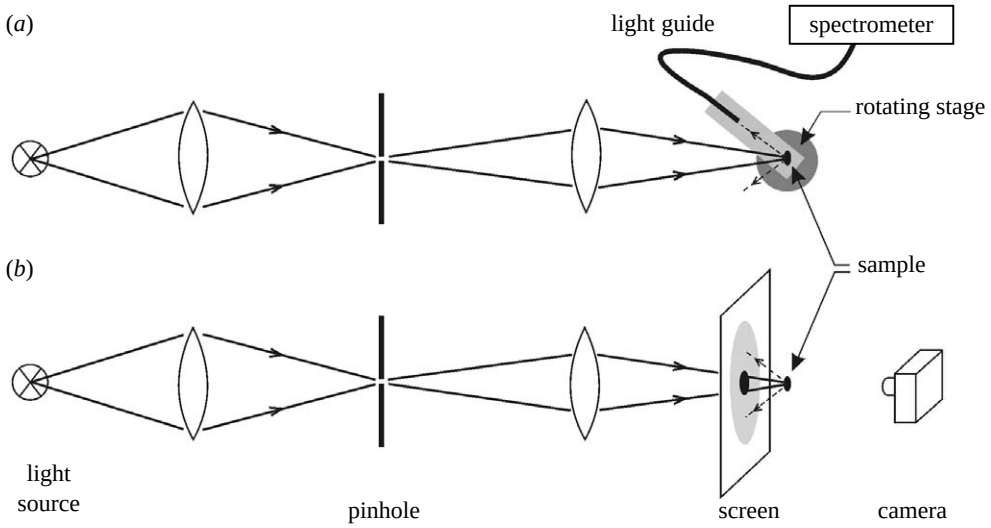

Figure 4. Diagram of an optical system for measuring the angular distribution of the light scattering from a sample. Light from a light source is focused on a pinhole, which is imaged on the sample. (*a*) The light scattered by the sample is collected at a range of polar angles by a light guide mounted on a rotating stage and delivered to a spectrometer. (*b*) A white screen with a small hole placed in between the imaging lens and the scale allows visualization of the spatial distribution of the light reflected by the butterfly scale; this may also be done in transmission (modified from Giraldo *et al.* 2008).

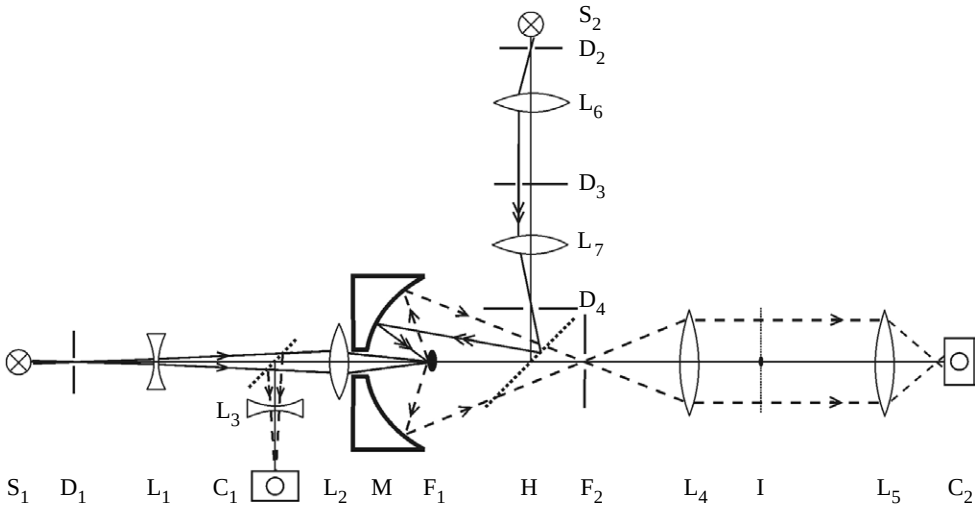

Figure 5. Imaging scatterometer. $S_{1,2}$, light sources; $L_{1–6}$, lenses; $D_{1–4}$, diaphragms; $C_{1,2}$, digital cameras; M, ellipsoidal mirror; $F_{1,2}$, focal points of the mirror; H, half-mirror. Light from S_1 creates a narrow aperture axial beam. Camera C_1 visualizes the sample and camera C_2 visualizes plane I, the back-focal plane of lens L_4, where the scattering pattern of the sample located in F_1 (black speck) is imaged and a spatial filter is placed to interrupt the first-order transmitted light. Light from S_2 passes the movable diaphragm D_3 in the front-focal plane of lens L_7, which thus creates a light beam with a variable incident angle. Diaphragm D_4 is in the back-focal plane of L_7, and is conjugated to a diaphragm in plane F_2 by half-mirror H.

barbule, is shown in figure 4*b*. A white screen with a small hole, placed in front of the light scattering sample, acting as a secondary scatterer, yields an immediate image of the spatial distribution of light reflected by the sample (Kinoshita *et al.* 2002; Yoshioka & Kinoshita 2006*a*; Giraldo *et al.* 2008). The pattern on the screen can be photographed, and then the spatial properties can be quantitatively analysed, for instance by correcting for the angular distortion of the flat screen. However, the camera captures only a minor fraction of the light scattered by the sample (figure 4*b*), and therefore the method is insensitive. To measure the scattering pattern as a function of the angle of incidence, the scale has to be rotated and additional screens have to be placed, but this approach has associated limitations (see Kinoshita *et al.* 2008). As discussed in the following, alternative methods are fortunately available.

3.2. Imaging scatterometry

Generally, it is very difficult to capture experimentally the data associated with the numerator in the BRDF formula shown in equation (2.1). This is in fact the hemispherical light intensity distribution of scattered light per unit surface area as a function of the polar and azimuthal angle, $I_r(\theta_r,\varphi_r)$. While it is not something that can be achieved with normal photographical methods, it is something that can be captured by the recently developed imaging scatterometer of figure 5 (see also

Stavenga *et al.* 2009; Wilts *et al.* 2009). Its central element is an ellipsoidal mirror, where the sample is mounted in the first focal point. Light from the principal source is focused at the sample via a small hole in the ellipsoid. The mirror folds hemispherically scattered light into a narrow cone that is accepted by a photographic lens. The far-field scattering pattern emerges in the back-focal plane of that lens, and that plane is imaged by a second lens on a digital camera. A secondary light path allows measurement of the scattering pattern as a function of the angle of incidence. Light from the secondary source passes a diaphragm, in the front-focal plane of a lens, which is, via a beam splitter, confocal with the second focal point of the ellipsoid. Varying the position of the diaphragm thus results in a varying angle of incidence of the light beam reaching the scale.

Figure 6 presents measurements performed with the imaging scatterometer on a single blue scale of a *Morpho aega* butterfly. Confirming previous measurements with the set-up of figure 4*b* (Kinoshita *et al.* 2002; Giraldo *et al.* 2008), upon perpendicular illumination, a *Morpho* scale reflects blue light into a narrow spatial strip (figure 6*f*). This intensity distribution pattern, which is matched by much earlier work on a large area of whole *Morpho* wing (Wright 1963), can be directly understood from the structuring of the scale ridges into slender multilayers (Vukusic *et al.* 1999; Kinoshita *et al.* 2002, 2008). Rotation of the scale results in a scattering pattern shifted towards shorter wavelengths (cf. figure 6*f* with *b* and *i*). This is entirely expected from a multilayer system. The iridescence, the illumination-dependent colour, is clearly observable on the reflecting wings of intact *Morpho* butterflies (Berthier 2003).

To determine the scattering patterns as a function of the wavelength, the light source can be filtered with interference filters or a monochromator, and a black-and-white camera can be used instead of a colour digital camera. From images taken at a series of wavelengths (multispectral imaging), reflectance spectra for each pixel, or spatial direction (θ_r,φ_r), can be derived, for instance using ImageJ (http://rsbweb.nih.gov/ij/). When the scale is rotated by an angle of $\pm 45°$, the scattered light escapes the hemisphere of the solid angle captured by the ellipsoid. For this reason, the scatterometer of figure 5 is equipped with a secondary beam to allow studying the scattering for all angles of incidence.

Although the scatterometer arrangement of figure 5 provides the benefit of access to quantifying a sample's BRDF, it is not without its costs. The ellipsoidal mirror, for instance, has to be of extremely high quality and the imaging is very sensitive to an accurate positioning of the sample in the ellipsoid's focal point. In many cases, a simpler approach based on epi-illumination microscopy is attractive.

3.3. Microscatterometry and microspectrophotometry

In the microscatterometer of figure 7, the sample is illuminated via a half-mirror and a microscope objective. The beam size and direction are determined by diaphragms under visual control via a photomicroscope, and the scattering pattern at infinity (i.e. projected in the back-focal plane of lens L_5 in figure 7) can then be photographed. Obviously, the objective aperture determines the spatial extent of both the illumination and scattering, but for objectives with numerical apertures as large as 0.85 or more, angles of approximately 60° can be achieved, allowing the imaging of scattering over a large spatial angle.

The dependence of the scattering pattern on wavelength can be studied with the microscatterometer using the method of multispectral imaging, as explained in §3.2, that is, by taking images with a series of illuminations at different wavelengths. Alternatively, the tip of a light guide, connected to a spectrometer, can be placed in plane I (figure 7*a*), so that then, using white light, the reflectance spectrum can be measured as a function of scattering direction.

The latter approach is analogous to epi-illumination microspectrophotometry. In this method, light from the reflecting sample reaches the image plane, where the tip of the spectrometer-connected light guide or, alternatively, an adjustable diaphragm in front of a photomultiplier tube is positioned. The measured reflectance spectra then are the integrated spectra over the objective aperture, so that the directional information is lost.

Reflectance spectra are usually measured with respect to a reference standard, so that the convolving effect of the characteristic wavelength dependence of the illuminant may be removed. This reference standard is usually a spectralon diffuse reflectance standard. It is, however, important to note that this can frequently lead to confusing and adverse results for structurally coloured objects. This is because the reflectance standard may scatter the incident light spatially very differently from the sample under investigation. Microspectrophotometrically measured reflectance spectra from natural samples may then often show reflectance values exceeding the value 100 per cent, unless special consideration is given to the nature of the sample. Quantified scattered light intensity measurements that appear to exceed the incident light intensity in this way reveal the potentially ambiguous nature of the measurements carried out.

3.4. Integrating sphere

An integrating sphere is used for integrating the radiant flux scattered from or through a sample over an entire hemisphere. The instrument is formed of a hollow sphere, which has its internal surface prepared with a diffusely reflective coating. For applications associated with investigating coloured samples, it generally features three openings or ports that are used for introducing light from the illuminant, presenting sample surfaces to that light and as an outlet for the light that is subsequently scattered (e.g. Andersson & Prager 2006). A fibre-optic-fed spectrometer is used to analyse this scattered light if the illuminant is a broadband source. Generally, the intensity of light inside an integrating sphere may be considered nearly uniform, because the multiple diffuse reflections from the sphere's interior wall reduce the introduced light's

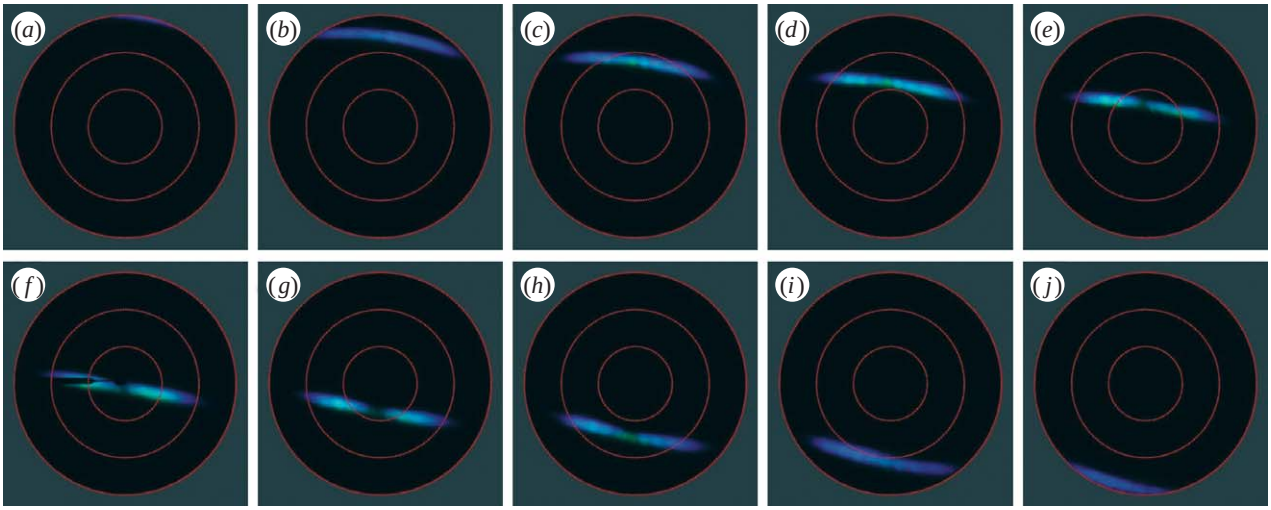

Figure 6. Scattering diagrams of a single *Morpho aega* wing scale created by the principal beam of the imaging scatterometer of figure 5. The scale was rotated in steps of 10° around a horizontal axis, about perpendicular to the ridges running longitudinally in the scale surface. The black strip at 270° in (*f*) is the shadow of a thin glass micropipette carrying the scale. The red circles indicate scattering angles of 30°, 60° and 90°.

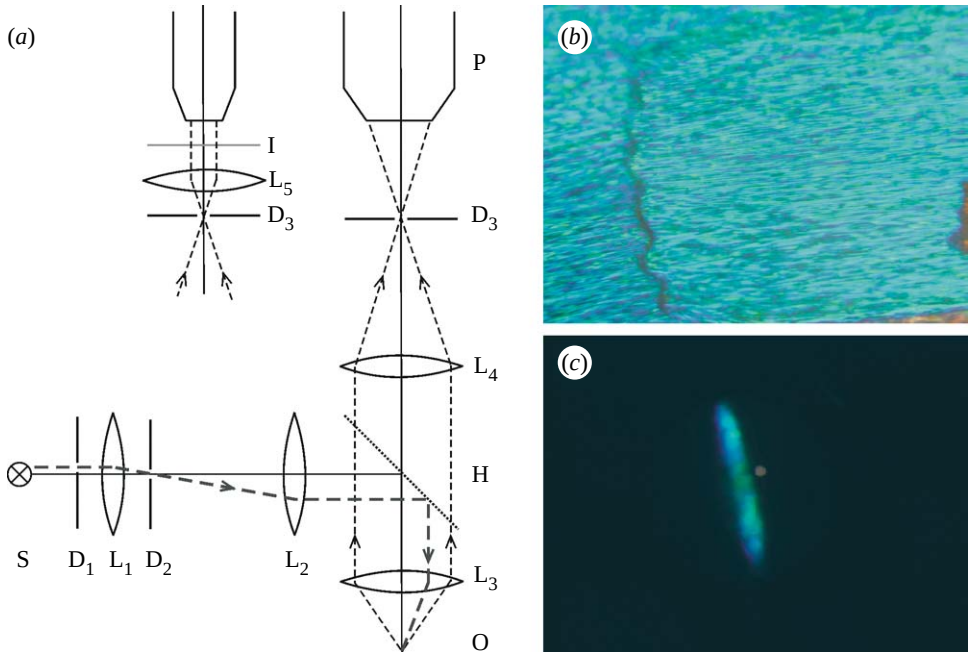

Figure 7. (*a*) Microscatterometer based on an epi-illumination microscope. All lenses, $L_{1–5}$, are confocal, thus forming telescopic systems. $D_{1–3}$, diaphragms; S, light source; H, half-mirror; O, sample; P, photomicroscope. A narrow light beam, restricted by diaphragms D_1 and D_2, reaches the sample O under a certain angle. The illumination spot is observable by focusing the photomicroscope at the plane of diaphragm D_3. By inserting lens L_5, the far-field (infinity) scattering pattern is observed in plane I, the back-focal plane of L_5 (modified from Stavenga 2002). (*b*) Part of a *M. aega* scale photographed with the right-hand arrangement of (*a*). (*c*) The associated far-field pattern photographed with the left-hand arrangement of (*a*).

angular dependence. As a result, every point on the sphere wall produces an equal light-field density per unit solid angle. Further effects of the multiple reflections are the removal of any short-time-scale temporal and polarization information associated with the incident or scattered light.

It is important to note that the light which is scattered from the sample will itself form a component of the light field within the sphere and will subsequently also interact with the sample. This leads to a scattered field measurement, which may be rather convolved. Similarly, the presence of two or three (or more) ports in the sphere also reduces the incident and scattered light fields, which further complicate any subsequent quantitative analysis. The same caution in the use of white reference surfaces for the calibration of the incident light, described previously, should be applied to the use of a white reference when using an integrating sphere. Despite these limiting factors, however, reflectance spectra measured with an integrating sphere can provide valuable information, especially for diffusively scattering materials (e.g. Ghiradella *et al.* 1972; Yoshioka & Kinoshita 2006*b*; Giraldo & Stavenga 2007).

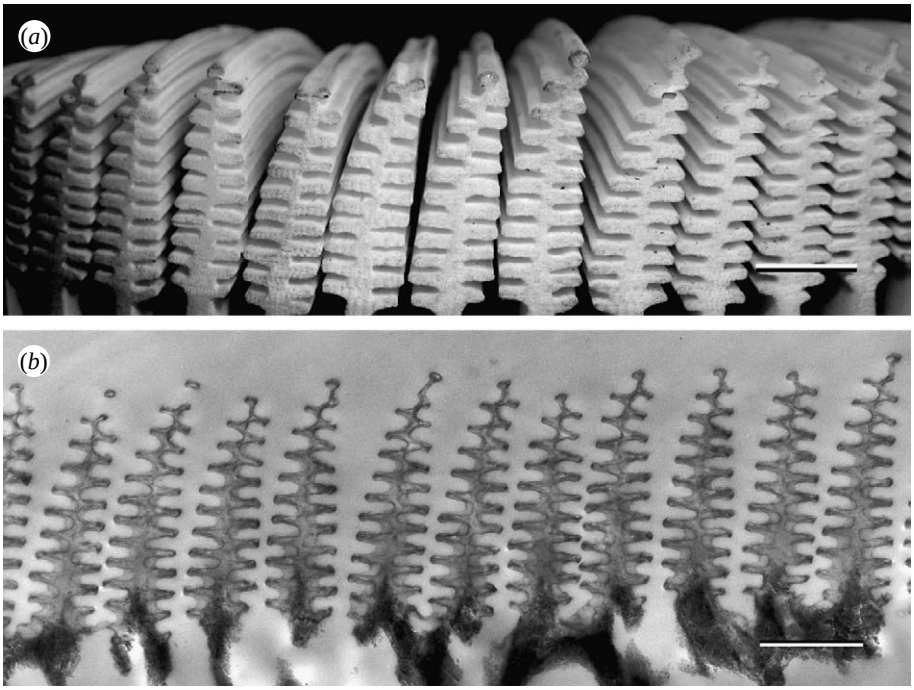

Figure 8. (*a*) Large replica model made of polymer and based explicitly on (*b*) the TEM cross section through a *Morpho rhetenor* butterfly wing scale. Scale bars: (*a*) 1.5 cm and (*b*) 800 nm.

3.5. Bifurcated flexible fibre-optic probe

A very useful and highly versatile, commercially available device is the bifurcated, flexible fibre-optic probe (for an extensive description, see Andersson & Prager (2006)). The fibre-probe comprises six light guides that can deliver the incident light to a surface and which collectively surround a central fibre that collects the scattered light and delivers it to a spectrometer. The numerical aperture of the device associated with the light it collects depends on the proximity of the tip to the surface. For a typical working distance of a few millimetres, the numerical aperture is then equivalent to a few degrees. The prevailing disadvantages of this technique, however, are associated with the poor resolution of spatial scattering characteristics. However, in situations where spectral reflectance information is at a premium, large datasets can be assembled quickly and at little cost.

Polarization characteristics are fully lost when using common optical fibres. The polarization state of the incident light has received little attention in all but a few studies on structural coloration. However, when polarization signalling is an important component of, say, an animal's communication channel, then measurement of the reflectance spectra and scattering profiles for different polarizations becomes necessary (Vukusic & Sambles 2001, 2003; Sweeney *et al.* 2003; Douglas *et al.* 2007; Yoshioka & Kinoshita 2007).

3.6. Scaled-up models for interrogation at microwave wavelengths

The experimental methods described so far often require the skilful physical manipulation and optical interrogation of micro- and nano-scale animal ultrastructures. For instance, the techniques for optically interrogating the single isolated scales of butterflies first require those individual scales to be appropriately separated from the wing substrate and mounted by their proximal tips onto adapted mechanical supports, such as ground-down needle tips or micropipettes (Vukusic *et al.* 1999; Giraldo *et al.* 2008; Kinoshita *et al.* 2008). There is the further complexity of optically probing and characterizing these small area samples (typical butterfly scales are approximately 150 μm × 75 μm). These procedures are not without difficulties and can come at a substantial cost in terms of limitations in the way in which the experimental variables, such as sample orientation and interrogated surface areas, may be selected.

An attractive alternative route is available by using high-magnification transmission electron microscopy (TEM) images of sample cross sections and subsequent laser-sintering or rapid-prototyping manufacturing processes as the basis of the replication of large-scale models (approx. 20 000 times larger). These models reproduce the natural sample nano- and micro-structures at the millimetre and centimetre scale out of polymer materials. They permit the exploration of the samples' optical properties using microwave wavelengths due to the scalability of electromagnetic scattering phenomena in the presence of analogous material properties. A first study, using this approach on the silver scales of the butterfly *Argyrophorus argenteus*, has been completed (Vukusic *et al.* 2009), and other scale models similar to that of the butterfly *Morpho rhetenor* (figure 8) are presently under investigation.

3.7. Light sources

For spectrometric investigations, the chosen light source should be suitably broadband and comprise appropriate intensity across the entire wavelength

range of interest. This intensity should either not fluctuate with time after a suitable warm-up period, or its fluctuation should be accounted for in data processing. Combined with a photodiode array spectrometer, a halogen–deuterium lamp may be used as a light source (Stavenga *et al.* 2006*a*). Alternatively, a (pulsed) Xe lamp may be used for spectrophotometry (Prum 2006; Yoshioka & Kinoshita 2006*b*; Rutowski *et al.* 2007). White light super-continuum sources have also been used to characterize aspects of *Morpho* butterfly appearance (Plattner 2004). However, while they provide excellent flat-band intensity from 500 nm upwards, their poorer output below 450 nm can hinder effective investigation of samples for which shorter wavelength characterization is a vital component.

For all broadband sources, the effect of their characteristic spectral profiles should be carefully removed by appropriately ratioing the spectra associated with the data by that of the light source. As has been mentioned previously, where a spectrum from a white reference surface is used in place of the spectrum associated directly with the light source itself, great care should be taken to account rigorously for discrepancies associated with wavelength-dependent absorption, polarization and intensity-related angle dependence of the reference. These variables may be to some degree manipulated by the reference standard.

For non-spectrometric investigations, the chosen light source may be a laser or a high-quality monochromator, the intensities and polarizations of which may be controlled with appropriate filters. Lasers have the advantage of delivering a considerable light flux, but they are spectrally limited to a discrete number of wavelengths.

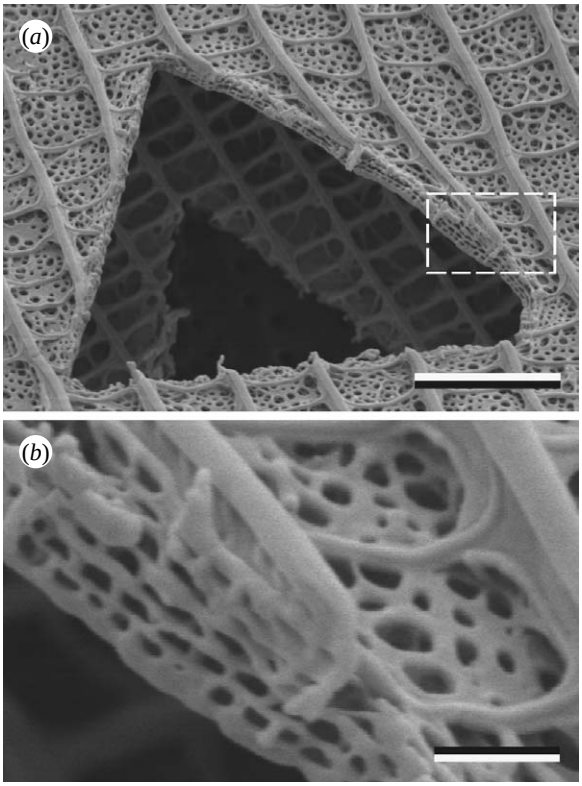

Figure 9. (*a*) A triangular hole cut into a cover and ground wing scale of the common grass blue (*Zizina labradus labradus*) with a focused-ion-beam scanning electron microscope (courtesy of Dr Sally Stowe, ANU, Canberra). (*b*) The area indicated by the dashed rectangle in (*a*). The cover scale lumen appears to consist of a four-tiered, perforated multilayer that scatters blue light (see Wilts *et al.* 2009). Scale bars: (*a*) 3 µm and (*b*) 0.5 µm.

4. STRUCTURAL METHODS

Physical understanding of the spatial and spectral data measured from structurally coloured biological samples inherently demands detailed knowledge of both the ultrastructure and the RI of the samples. Light microscopy is generally not suitable for gathering this structure information since the associated periodicities are generally in the range of 50–500 nm. Electron microscopy is therefore an indispensable tool, since with appropriate sample preparation, it enables imaging of the crucial structures that determine the structural colours.

4.1. Scanning electron microscopy

A direct and generally straightforward way to gain some insight into structures that create structural colour in biological systems with micrometre and nanometre dimensions is through use of scanning electron microscopy (SEM). However, while SEM generally shows surface profiles and features, its usefulness may be limited with certain samples, because the ultrastructure responsible for biological structural colour is very often subsurface. Therefore, when using SEM, it is necessary to induce or expose mechanically a cross section in the sample. This may be carried out with sharp razor blades or by using either commercial cryosectioning or freeze–fracture facilities. A more controlled preparation method is offered by focused-ion-beam SEM (FIBSEM). With this facility, the directed ion beam incises the material along a chosen direction and at a chosen rate, so that it becomes possible to observe the exposed section profile (figure 9).

The FIBSEM technique has been used for the examination of scattering bead structures on the scales of pierid butterflies (Stavenga *et al.* 2004; Smentkowski *et al.* 2006). More recently, Galusha *et al.* (2008) have used FIBSEM in an elegant, alternative procedure. In their study on the photonics of the weevil *Lamprocyphus augustus*, they took a series of SEM pictures from the cuticle, after sectioning consecutive thin layers and resputtering each newly exposed surface for SEM. This enabled reconstruction of the diamond-like structure that causes the weevil's intense green iridescence. This method is somewhat analogous to the procedure applied in TEM, one of the key methods for studying the anatomy of a biological system.

4.2. Transmission electron microscopy

Imaging using TEM methods can be of fundamental importance for studying samples, the subsurface fine structure of which creates their structural colour

properties. As a method, however, it requires considerable effort and expertise when compared with SEM. The material must be fixed, stained and embedded in a suitable resin that allows extremely thin (typically 70 nm thick) sectioning. Insight into the three-dimensional structure of the material may then be deduced from images of a series of sections. On occasion, the complete three-dimensional architecture of a sample may be inferred using appropriate computer modelling and a series of high-quality good TEM images, even from sections whose thickness may be less than the periodicity of the structure (Michielsen & Stavenga 2008).

An alternative approach can also lead to virtual reconstruction of the three-dimensional model. TEM tomography is a widely applied technique that can image relatively large structures of various types; periodic or aperiodic. A series of TEM images that is tilted sequentially over many different tilt angles about one axis can be combined tomographically to reconstruct a virtual three-dimensional model that is based explicitly on the original three-dimensional structure of the sample. This method was trialled on the wing scales of the Kaiser-I-Hind butterfly (*Teinopalpus imperialis*) structure (Argyros *et al.* 2002).

In the case of simpler multilayer structures, like those of damselfly wing-cell membranes (figure 10), straightforward TEM imaging may yield the dimensions of a sample's constituent layers. These then may be used to predict the wing reflectance spectra (Vukusic *et al.* 2004).

4.3. Atomic force microscopy

The three-dimensional profile of the intact surface of a sample can be quantitatively determined by atomic force microscopy (AFM). This method has been applied to the corneal nipple array of moth eyes, where the surface structure counteracts reflections (Stavenga *et al.* 2006*b*). The applicability to structurally coloured biological systems is limited, however, because AFM is unable to probe structures beneath the outer surface of a sample.

4.4. Refractive index measurements

In addition to the structure, the RI of the material determines its structural colour. Although the classical methods of refractometry are not applicable to materials with structural colours, there are alternatives. The simplest one, applying suitable immersion fluids with known refractive indices, can be applied when the material has an open structure and the immersion fluid can permeate through its air-filled spaces. This is the case for many butterfly wing scales. The reflection vanishes when the immersion fluid has a RI approaching that of the material (Nijhout 1991; Vukusic *et al.* 1999; Berthier 2003; Stavenga *et al.* 2004). Of course, the immersion method only works when the RI is constant throughout the sample. Fortunately, this seems to hold for many butterfly wing scales, which have chitin as their main constituent, with a RI of 1.56 (Vukusic *et al.* 1999). Damselfly wings have layers with lower (1.47) as well as higher (1.68 and 1.74) real refractive indices (Vukusic *et al.* 2004).

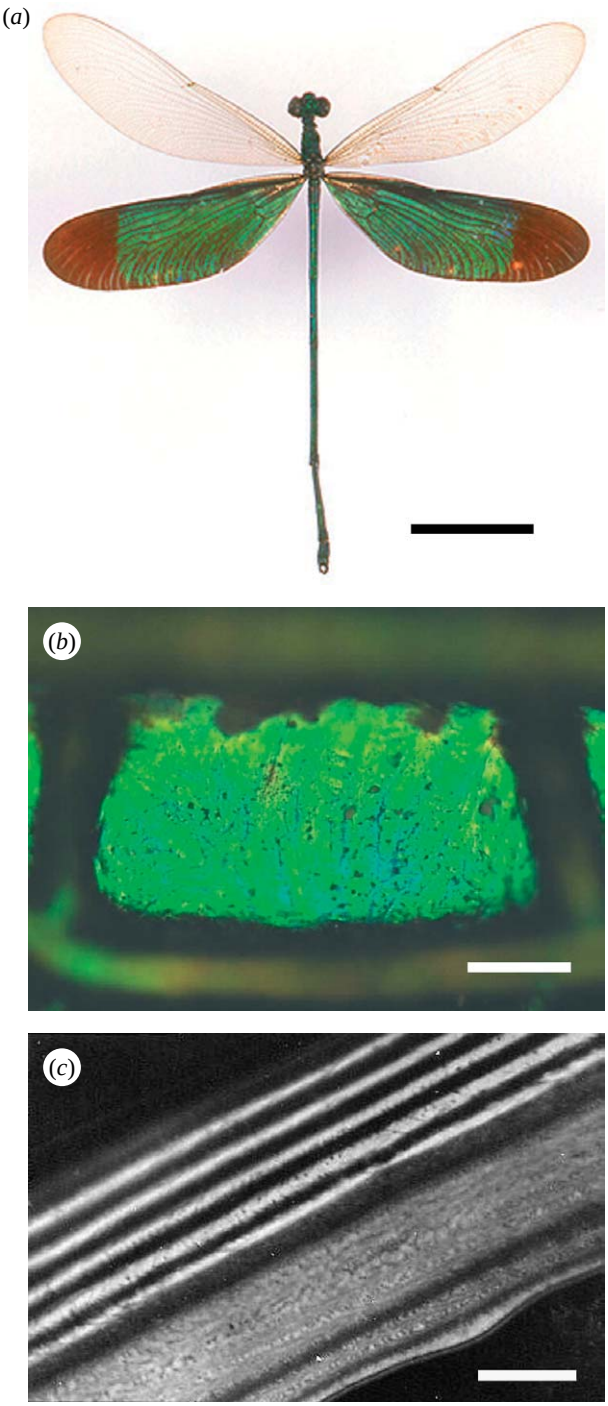

Figure 10. (*a*) The damselfly *Neurobasis chinensis* exhibits bright and highly saturated iridescent green hind wings as a result of the melanin-backed multilayer in its (*b*) wing membrane. (*c*) TEM images resolve the periodic spatial variation in the constituent material. Scale bars: (*a*) 1 cm, (*b*) 5 μm and (*c*) 0.5 μm.

Interestingly, the RI changes in a subtle way when vapours adhere to *Morpho* wing scales, causing a change in reflectance. This phenomenon can be exploited in extremely sensitive RI measurements (Portyrailo *et al.* 2007; Biró *et al.* 2008).

A complicating factor is that structurally coloured biological systems almost universally contain absorbing pigments, notably the melanins (Fox & Vevers 1960). The presence of melanin in a sample increases

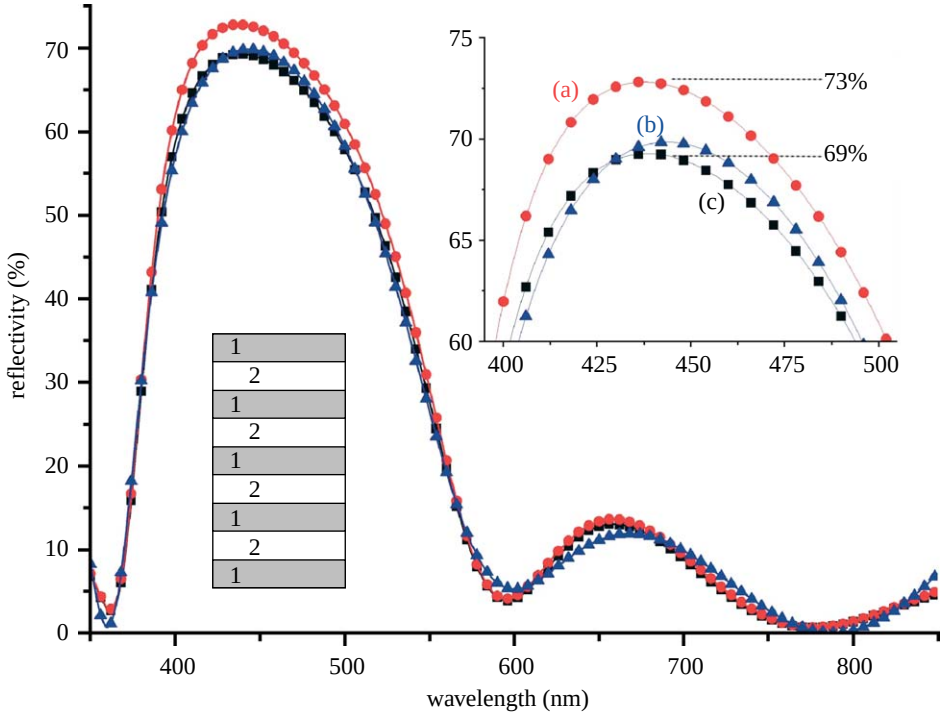

Figure 11. Three very similar reflectance spectra modelled for a multilayer with very different parameters. (a) Refractive indices $n_1=1.56+0.06i$ and $n_2=1.00$; and nine layers (see inset) with alternating $d_1=80$ nm and $d_2=100$ nm. (b) Refractive indices $n_1=1.56+0.06i$, $n_2=1.00$; and nine layers with thicknesses 53, 134, 77, 90, 83, 105, 77, 90 and 89 nm, respectively. (c) Refractive indices $n_1=1.83+0.06i$ and $n_2=1.12$; and seven layers with thicknesses 81, 58, 41, 184, 55, 52 and 87 nm, respectively.

both the real and imaginary parts of its RI. Unfortunately, the RI of melanin is poorly documented. In numerous studies, the real part of the RI of melanin-containing material is taken to be 2.0 (e.g. Durrer & Villiger 1970; Schultz & Rankin 1985; Zi *et al.* 2003; Brink & van der Berg 2004). This value, however, has no solid experimental basis, and thus urgently needs reassessment. The imaginary component of the RI of *Morpho* butterfly scales, due to melanin, was determined to be approximately 0.06, and for damselfly wings values as high as 0.13 were derived (Vukusic *et al.* 2004).

Melanin granules play a key role in the coloration of feathers of many bird species. The granules are arrayed into photonic structures, which often resemble multilayers, but sometimes take up more intricate arrangements (Durrer & Villiger 1970; Durrer 1977, 1986; Prum 2006; Kinoshita *et al.* 2008).

5. THEORETICALLY MODELLING STRUCTURAL COLORATION

5.1. Single thin films

The most accessible theoretical model is that for optical interference effects in a thin layer (Kinoshita *et al.* 2008). The green and purple colours of the neck feathers of the rock dove, *Columba livia*, were explained in great detail by Yoshioka *et al.* (2007), by assuming that the cortex of the barbules acts as an optical thin film and that the numerous pigment granules in the core of the barbules function as an absorbing base layer (for a similar treatise of *Hadeda ibis* feathers, see Brink & van der Berg (2004)).

5.2. Multilayer thin films

The theoretical reflectance or transmittance spectrum of a real multilayer system can be directly calculated with a matrix formalism method when the dimensions of its constituent layers and the values of their complex refractive indices are known (Macleod 1986; Jellison 1993; Yeh 2005). In practice, the multilayer parameters may be adjusted until the theoretically predicted spectrum matches the associated experimentally measured spectrum. When the two spectra closely match for realistic layer thicknesses and refractive indices, the system's optical processes are deemed well understood. For this practice to occur successfully, however, it is essential that the optical measurements are completed as accurately as possible, and also that the subsequent interpretation of the theory that is generated to match experiment proceeds with caution.

We present the following as an example of the need for such caution. The three reflectance spectra of figure 11 are associated with a hypothetical butterfly's structurally coloured appearance. They have all been generated theoretically. The peak reflectances of all three datasets are extremely close (system (a) peaks at 73%, (b) at 70% and (c) at 69%). Spectrum (a) is generated by typical, albeit unsophisticated, lepidopteran scale parameters (see the caption to figure 11 for details). The spectra for systems (b) and (c) are extremely similar to spectrum (a); however, their associated parameters (i.e. layer thicknesses and refractive indices) are completely unrealistic as structural and material parameters of a lepidopteran system.

The significance of this, therefore, is that if the reflectance spectra measured from a structurally

coloured surface has an error in the peak value of even a few per cent due, for instance, to the limitations of the optical technique employed, then it will not be possible to discriminate between many potential solutions with any associated theoretical modelling. Reliable modelling is much more successfully executed with large numbers of experimental datasets; for instance, when the reflectance or transmittance spectra are measured on the same sample for a variety of angles of incidence at different linear polarizations (e.g. Vukusic *et al.* 2004; Noyes *et al.* 2007).

Multilayers exist in the exocuticle of many species, including birds, beetles and damselflies (e.g. Kurachi *et al.* 2002; Prum 2006; Vigneron *et al.* 2006; Land *et al.* 2007; Kinoshita *et al.* 2008). The layers are seen in TEM images of these species' cross sections as alternating layers of greyscale that are associated with regions which are more or less electron dense. This is presumed to originate either from a varying concentration in each layer of the light-absorbing pigment melanin, which is assumed to have electron-dense properties, or from the varying levels of uptake by melanin molecules of the heavy metal stains applied during the TEM sample preparation process (Vukusic *et al.* 2001). The published models of beetle reflectance spectra (Kurachi *et al.* 2002; Hariyama *et al.* 2005) have not incorporated complex refractive indices, however.

Multilayer modelling with complex refractive indices indicates that the main effect of the imaginary component is a reduction of the reflectance. The shape of the reflectance spectrum is strongly dependent on the RI contrast, i.e. the ratio between the (real part of the) refractive indices of adjacent layers (Kinoshita *et al.* 2008; Wilts *et al.* 2009). Although simplified, multilayer-based interpretations have been put forward for explaining bird feather colorations (Durrer 1977, 1986; Doucet *et al.* 2006), they are probably not adequate for explaining the observed spatial and spectral reflectance characteristics, because of the intrinsic structure which incorporates aspects of two- and three-dimensional RI variation.

5.3. Three-dimensional photonic crystals

Three-dimensional-ordered or quasi-ordered structures with appropriately sized spatial variations in RI underpin the structural colours associated with a range of different species across many different animal species, notably birds and butterflies, but also many beetles (Durrer 1977; Vukusic & Sambles 2003; Welch 2005; Prum 2006; Galusha *et al.* 2008). Natural photonic structures with three-dimensional periodicity appear first to have been identified in some detail among the lepidoptera (Morris 1975) and were originally thought to be rather rare, but are now found with increasing frequency. Although their optical behaviour was originally well understood at a conceptual level, the photonics modelling processes that were available at the time were insufficiently advanced to enable formal theoretical treatments. More recently, with improvements in computing facilities and the development of the field of photonics in technological systems, theoretical modelling methods, by which natural three-dimensional-ordered systems may now be considered, are much more available. As a result of this, insight into the behaviour and photonic performance of natural three-dimensional periodic systems is now much more accessible and their systems are better understood.

Several procedures have been developed with which such systems may be modelled. The method of Johnson & Joannopoulos (2001) comprises an iterative frequency-domain process that uses a vectorial, three-dimensional algorithm to compute the definite-frequency eigenstates of Maxwell's equations in periodic dielectric structures. It is available and widely used as a free computer program downloadable from the Web (MIT Photonic-Bands Package; http://ab-initio.mit.edu/mpb/). Many other computer modelling procedures have been successfully developed over the last decade and applied to this field by individual research groups and commercial software organizations. This includes many variations on the adaptable and widely used finite-difference time-domain method (Plattner 2004; Taflove & Hagness 2005) and also the finite-element method applied to electromagnetics (e.g. the HFSS solver by Ansoft Inc. and the RF modelling module by the Comsol Group).

A range of investigations have formally considered natural three-dimensional-ordered or quasi-ordered structures. The reflectance spectra of biological three-dimensional photonic crystals have been calculated for structurally coloured peacock feathers by Zi *et al.* (2003) and Li *et al.* (2005; see also Yoshioka & Kinoshita 2002). Various investigations have examined and theoretically treated the three-dimensional systems in the elytral and body scales of weevils (e.g. Welch *et al.* 2007; Galusha *et al.* 2008). The photonic properties of the ultrastructure of a centric species of diatom, *Coscinodiscus granii*, were theoretically investigated by Fuhrman *et al.* (2004), and the optical properties of the periodic structure within the iridescent setae of a polychaete worm have been modelled by McPhedran *et al.* (2003).

Most of these and the existing theoretical treatments, however, have invariably generalized the exact spatial geometry and structural profiles of the modelled three-dimensional structures. The refractive indices used, too, have routinely been based on qualified assumptions and estimates, which in many cases have lacked rigorous experimental verification. These are key areas of weakness throughout the field of photonics of natural structures. Furthermore, most theoretical treatments may imperfectly represent the often very limited number of spatial periods in a real system, modelling the systems instead as being continuously periodic. Also, the existence, in very many three-dimensional ordered systems, of neighbouring domains of randomly oriented regions of periodic structure has not been theoretically treated in great detail, although experimental evidence of their effect in real systems suggests that they produce structural colour that is largely absent of angle-dependent hue effects (Vukusic & Sambles 2003). To date, therefore, despite significant recent progress, highly accurate quantitative theoretical calculations of the spatial scattering

JOURNAL OF THE ROYAL SOCIETY Interface
JOURNAL OF THE ROYAL SOCIETY Interface

Table 1. Outline summary, including capabilities, limitations and key experimental variables, of the principal physical methods for the investigation of structural colour in biological systems.

technique	capabilities	limitations	key experimental variables
spectrophotometry (including microspectrophotometry and bifurcated fibre probe use)	used for measuring optical scattering from or through samples; polarized or unpolarized illumination can be provided with broadband or laser sources and appropriate filters; sample orientation and light incidence angle can usually be controlled; light can be delivered using optical fibres or conventional lenses; detection of scattered light achieved using fibre-fed spectrometers (for white light illumination) or large-area photodiodes (for laser or monochromatic light illumination)	difficult to measure absolute values of reflectance or transmittance; great care should be taken when using white reference standards; use of microspectrophotometer or bifurcated fibre probe precludes independent variation of angles of light incidence and scatter detection	incident and scattered light wavelengths; angle of incidence; scattered light detection angle; sample orientation; incident and scattered light polarization state; incident and scattered light intensities
integrating sphere photometry	used for measuring optical scattering from or through samples; light delivered using optical fibres or conventional lenses (dependent on sphere design); detection of scattered light achieved using fibre-fed spectrometers (for white light illumination) or large-area photodiodes (for laser or monochromatic light illumination; dependent on sphere design)	sample orientation and the illumination and scattered light detection angles are not selectable; there is no polarization selectivity; great care should be taken when using white reference standards	incident and scattered light wavelengths; incident and scattered light intensities
scatterometry and reflectometry	used for measuring scattered light distribution by applying point source illumination, the direction of which can be varied; detection can be realized with scanning fibres connected to a photodiode array spectrophotometer or by imaging	measurements with scanning fibres are extremely laborious; imaging methods require special optical methods when large spatial angles are to be spanned	the measured bidirectional reflectance distribution function involves knowledge of spatial directions of incident and scattered light, wavelength, polarization
scaled model fabrication and electromagnetic interrogation	used for replicating accurate millimetre- and centimetre-scale models appropriate for interrogation using much longer wavelengths (e.g. microwaves); replication processes are variable, but can include rapid prototyping and laser sintering; large-scale models are much easier to position and manipulate accurately; for biomimetic application studies, the models may be fabricated using one or more of a wide range of dielectric, semiconductor or metallic materials	the material used to replicate large-scale models should have analogous optical properties to the original optical sample	incident and scattered light wavelengths; angle of incidence; scattered light detection angle; sample orientation; incident and scattered light polarization state; incident and scattered light intensities
SEM	used for imaging the surfaces or exposed interiors of samples; typical available resolutions are a few nanometres to tens of nanometres; samples may be pre-prepared with an FIB procedure, freeze–fracture or mechanically induced damage to reveal subsurface structures; estimated dimensions of samples' surface nanostructure	owing to two-dimensional perception issues, SEM offers much less accuracy than TEM in quantifying dimensions of subsurface structures; poor sample preparation may lead to low image quality owing to electrical charging issues	orientation of the sample on the SEM stub; metal overlayer thickness; sample stub orientation in SEM; working distance; beam current and voltage; SEM detector mode (e.g. backscattered, secondary electrons)

(*Continued.*)

Table 1. (*Continued.*)

technique	capabilities	limitations	key experimental variables
TEM	used for imaging ultramicrotomed samples' thin (approx. 70 nm thick) sections; typical available resolutions are a few nanometres to tens of nanometres; different staining processes create differential greyscale contrast in the sample's nanostructure; accurate quantification of nano-structured dimensions and structural geometries is possible	ultramicrotome facilities and expertise with biophotonic sample sectioning have limited availability; poor sample fixing and staining protocols, in addition to poor sectioning technique may lead to artificial results	sample preparation fixative, impregnation and staining chemicals; ultramicrotome section thicknesses and orientations; TEM E-beam spot diameter and voltage
AFM	used for forming digital maps of samples' surface features; enables estimates of large area surface height distributions, which is not accurately possible with either SEM or TEM	does not work accurately for samples that exhibit features with significant height-to-separation ratios, or with crevice-like or partially covered subsurface features	operating mode (e.g. contact mode, tapping mode, etc.); probe-tip profile

properties of natural three-dimensional periodic systems are yet to be formally reported. This is principally because the exact structural geometries and material compositions of most natural three-dimensional periodic systems are not yet known in highly resolved detail. Some effort has been made to improve knowledge of species' exact structural geometries. As noted, Argyros and co-workers used TEM tomography to try to reconstruct digitally the unit cell of the three-dimensional structure of the butterfly *T. imperialis* (Argyros *et al.* 2002). Michielsen & Stavenga (2008) used an alternative method in which appropriately thin sections through computer three-dimensional crystal models were compared with TEM cross sections from various butterfly species, and concluded that the three-dimensional structures were gyroidal.

Prum and co-workers adopted an alternative approach to modelling. They used two-dimensional fast Fourier analysis of TEM images of some birds' feathers and also some insect scales and epicuticles to model the effect of the order and quasi-order in the animals' spatial RI variations (Prum *et al.* 1999, 2004, 2006; reviewed by Prum 2006). This method enables prediction of the distribution of momentum-space scattering centres associated with these systems that coherently scatter specific bands of wavelengths preferentially. However, presumably because two-dimensional TEM cross-sectional images of the samples' cross sections do not capture their ultrastructural information in all three dimensions, and also owing to the same uncertainties in material compositional parameters that affect other modelling approaches, the reflectance spectra they predicted have on occasion been limited in their correlation with the associated experimental observations.

There remain significant challenges in this area with all forms of theoretical modelling. With the onset of greater knowledge of material and structural parameters of various natural systems, most especially those with three-dimensional order or quasi-order to their structure, theoretical models will emerge that can consistently achieve far better agreement between calculations and experimental data than is currently available. With the exception of all but a very few studies, high-quality agreement in this respect has so far been incomplete.

6. CONCLUSIONS AND SUMMARY

A significant number of investigative approaches and experimental methods have been applied over the years to the study of structural colour effects in animals. It is clear, however, that no single technique can elicit all of the experimental information about the structurally coloured appearance of an animal system that would, by itself, be sufficient for complete understanding of its photonic character. Investigative techniques appear best used in complementary roles; generally, with optical and electron microscopy imaging methods complementing one or more spectrally resolved photometric reflection, transmission and, if possible, absorption measurements. Many of the key details of these methods have been summarized in this paper (table 1)

alongside descriptions of a small range of the seminal studies that have introduced advances in, or which have particularly successfully used, the methods themselves.

For a newly undertaken study on a previously uncharacterized sample, the choice of appropriate investigative techniques, beyond those of basic imaging, very much appears to depend on the sample's constituent material, its natural local environment, its size and its inherent optical character. For example, the appropriate methods for the detailed and complete photonic study of brightly coloured butterfly scales would, beyond basic imaging processes, be dissimilar to the appropriate methods for the study of cuttlefish appearance or that of white diffusely scattering beetle elytra. It is crucial that the scientist who undertakes an investigation in this area is informed of, and familiar with, the range of physical methods that are available. In this way, the use of appropriate techniques may be planned, established and then exploited so that a suitably broad range of photonic information about the biological system can be collected, processed and unlimitedly understood.

REFERENCES

Andersson, S. & Prager, M. 2006 Quantifying colors. In *Bird coloration*, vol. I (eds G. E. Hill & K. J. McGraw), pp. 41–89. Cambridge, MA: Harvard University Press.

Argyros, A., Manos, S., Large, M. C. J., McKenzie, D. R., Cox, G. C. & Dwarte, D. M. 2002 Electron tomography and computer visualisation of a three-dimensional 'photonic' crystal in a butterfly wing-scale. *Micron* **33**, 483–487. (doi:10.1016/S0968-4328(01)00044-0)

Berthier, S. 2003 *Iridescences, les couleurs physiques des insectes*. Paris, France: Springer.

Biró, L. P., Kertész, K., Vértesy, Z. & Bálint, Zs. 2008 Photonic nanoarchitectures occurring in butterfly scales as selective gas/vapor sensors. *Proc. SPIE* **7057**, 705 706. (doi:10.1117/12.794910)

Brink, D. J. & van der Berg, N. G. 2004 Structural colours from the feathers of the bird *Bostrychia hagedash*. *J. Phys. D: Appl. Phys.* **37**, 813–818. (doi:10.1088/0022-3727/37/5/025)

Doucet, S. M., Shawkey, M. D., Hill, G. E. & Montgomerie, R. 2006 Iridescent plumage in satin bowerbirds: structure, mechanisms and nanostructural predictors of individual variation in colour. *J. Exp. Biol.* **209**, 380–390. (doi:10.1242/jeb.01988)

Douglas, J. M., Cronin, T. W., Chiou, T. H. & Dominy, N. J. 2007 Light habitats and the role of polarized iridescence in the sensory ecology of neotropical nymphalid butterflies (Lepidoptera: Nymphalidae). *J. Exp. Biol.* **210**, 788–799. (doi:10.1242/jeb.02713)

Durrer, H. 1977 Schillerfarben der Vogelfeder als Evolutionsproblem. *Denkschr. Schweiz. Naturforsch. Ges.* **91**, 1–127.

Durrer, H. 1986 The skin of birds: colouration. In *Biology of the integument*, vol. 2: *Vertebrates* (eds J. Bereiter-Hahn A. G. Matoltsy & K. Sylvia Richards), pp. 239–247. Berlin, Germany: Springer.

Durrer, H. & Villiger, W. 1970 Schillerradien des Goldkuckucks (*Chrysococcyx cupreus* (Shaw)) im Elektronenmikroskop. *Z. Zellforsch.* **109**, 407–413. (doi:10.1007/BF02226912)

Forbes, P. 2006 *The gecko's foot: bio-inspiration—engineering new materials from nature*. London, UK: W.W. Norton.

Fox, H. M. & Vevers, G. 1960 *The nature of animal colours*. London, UK: Sidgwick and Jackson.

Fuhrmann, T., Landwehr, S., El Rharbi-Kucki, M. & Sumper, M. 2004 Diatoms as living photonic crystals. *Appl. Phys. B* **78**, 257–260. (doi:10.1007/s00340-004-1419-4)

Galusha, J. W., Richey, L. R., Gardner, J. S., Cha, J. N. & Bartl, M. H. 2008 Discovery of a diamond-based photonic crystal structure in beetle scales. *Phys. Rev. E* **77**, 050 904. (doi:10.1103/PhysRevE.77.050904)

Ghiradella Hairs, H. 1998 bristles, and scales. In *Microscopic anatomy of invertebrates*, vol. 11A (ed. M. Locke), pp. 257–287. New York, NY: Wiley-Liss.

Ghiradella, H., Aneshensley, D., Eisner, T., Silberglied, R. & Hinton, H. E. 1972 Ultraviolet reflection of a male butterfly: interference color caused by thin-layer elaboration of wing scales. *Science* **178**, 1214–1217. (doi:10.1126/science.178.4066.1214)

Giraldo, M. A. & Stavenga, D. G. 2007 Sexual dichroism and pigment localization in the wing scales of *Pieris rapae* butterflies. *Proc. R. Soc. B* **274**, 97–102. (doi:10.1098/rspb.2006.3708)

Giraldo, M. A., Yoshioka, S. & Stavenga, D. G. 2008 Far field scattering pattern of differently structured butterfly scales. *J. Comp. Physiol. A* **194**, 201–207. (doi:10.1007/s00359-007-0297-8)

Hariyama, T., Hironaka, M., Takaku, Y., Horiguchi, H. & Stavenga, D. G. 2005 The leaf beetle, the jewel beetle, and the damselfly; insects with a multilayered show case. In *Structural color in biological systems—principles and applications* (eds S. Kinoshita & S. Yoshioka), pp. 153–176. Osaka, Japan: Osaka University Press.

Jellison Jr, G. E. 1993 Data analysis for spectroscopic ellipsometry. *Thin Solid Films* **234**, 416–422. (doi:10.1016/0040-6090(93)90298-4)

Johnson, S. G. & Joannopoulos, J. D. 2001 Block-iterative frequency-domain methods for Maxwell's equations in a planewave basis. *Opt. Express* **8**, 173–190.

Kinoshita, S. & Yoshioka, S. 2005 Structural colors in nature: the role of regularity and irregularity in the structure. *ChemPhysChem* **6**, 1–19. (doi:10.1002/cphc.200490060)

Kinoshita, S., Yoshioka, S. & Kawagoe, K. 2002 Mechanisms of structural colour in the *Morpho* butterfly: cooperation of regularity and irregularity in an iridescent scale. *Proc. R. Soc. B* **269**, 1417–1421. (doi:10.1098/rspb.2002.2019)

Kinoshita, S., Yoshioka, S. & Miyazaki, J. 2008 Physics of structural colors. *Rep. Prog. Phys.* **71**, 076 401. (doi:10.1088/0034-4885/71/7/076401)

Kurachi, M., Takaku, Y., Komiya, Y. & Hariyama, T. 2002 The origin of extensive colour polymorphism in *Plateumaris sericea* (Chrysomelidae, Coleoptera). *Naturwissenschaften* **89**, 295–298. (doi:10.1007/s00114-002-0332-0)

Land, M. L., Lim, M. L. M. & Li, D. 2007 Optics of the ultraviolet reflecting scales of a jumping spider. *Proc. R. Soc. B* **274**, 1583–1589. (doi:10.1098/rspb.2007.0328)

Li, Y., Lu, Z., Yin, H., Yu, X., Liu, X. & Zi, J. 2005 Structural origin of the brown color of barbules in male peacock tail feathers. *Phys. Rev. E* **72**, 10 902. (doi:10.1103/PhysRevE.72.010902)

Macleod, H. A. 1986 *Thin-film optical filters*. Bristol, UK: Adam Hilger.

Marschner, S. R., Jensen, H. W., Levoy, M. & Hanrahan, P. 2001 A practical model for subsurface light transport. In *Proc. SIGGRAPH*, pp. 511–518. Los Angeles, CA: ACM Press.

Mason, C. W. 1926 Structural colors in insects. 1. *J. Phys. Chem.* **30**, 383–395. (doi:10.1021/j150261a009)

Mason, C. W. 1927 Structural colors in insects. 2. *J. Phys. Chem.* **31**, 321–354. (doi:10.1021/j150273a001)

McPhedran, R. C., Nicorovici, N.-A.P., McKenzie, D. R., Rouse, G. W., Botten, L. C., Welch, V., Parker, A. R., Wohlgennant, M. & Vardeny, V. 2003 Structural colours through photonic crystals. *Phys. B: Condens. Matter* **338**, 182–185. (doi:10.1016/S0921-4526(03)00483-6)

Michielsen, K. & Stavenga, D. G. 2008 Gyroid cuticular structures in butterfly wing scales: biological photonic crystals. *J. R. Soc. Interface* **5**, 85–94. (doi:10.1098/rsif.2007.1065)

Morehouse, N. I., Vukusic, P. & Rutowski, R. 2007 Pterin pigment granules are responsible for both broadband light scattering and wavelength selective absorption in the wing scales of pierid butterflies. *Proc. R. Soc. B* **274**, 359–366. (doi:10.1098/rspb.2006.3730)

Morris, R. B. 1975 Iridescence from diffraction structures in the wing scales of *Callophrys rubi*, the Green Hairstreak. *J. Entomol. Ser. A* **49**, 149–154.

Nicodemus, F. E. 1965 Directional reflectance and emissivity of an opaque surface. *Appl. Opt.* **4**, 767–773. (doi:10.1364/AO.4.000767)

Nicodemus, F. E., Richmond, J. C., Hsia, J. J., Ginsberg, I. W. & Limperis, T. 1977 *Geometric considerations and nomenclature for reflectance*. Monograph, no. 161. National Bureau of Standards (US).

Nijhout, H. F. 1991 *The development and evolution of butterfly wing patterns*. Washington, DC: Smithsonian Institution Press.

Noyes, J. A., Vukusic, P. & Hooper, I. R. 2007 Experimental method for reliably establishing the refractive index of buprestid beetle exocuticle. *Opt. Express* **15**, 4351–4358. (doi:10.1364/OE.15.004351)

Plattner, L. 2004 Optical properties of the scales of *Morpho rhetenor* butterflies: theoretical and experimental investigation of the back-scattering of light in the visible spectrum. *J. R. Soc. Interface* **1**, 49–59. (doi:10.1098/rsif.2004.0006)

Potyrailo, R. A., Ghiradella, H., Vertiatchikh, A., Dovidenko, K., Cournoyer, J. R. & Olson, E. 2007 *Morpho* butterfly wing scales demonstrate highly selective vapour response. *Nat. Photonics* **1**, 123–128. (doi:10.1038/nphoton.2007.2)

Prum, R. O. 2006 Anatomy, physics, and evolution of structural colors. In *Bird coloration*, vol. I (eds G. E. Hill & K. J. McGraw), pp. 295–353. Cambridge, MA: Harvard University Press.

Prum, R. O., Torres, R. H., Williamson, S. & Dyck, J. 1999 Two-dimensional Fourier analysis of the spongy medullary keratin of structurally coloured feather barbs. *Proc. R. Soc. B* **266**, 13–22. (doi:10.1098/rspb.1999.0598)

Prum, R. O., Cole, J. A. & Torres, R. H. 2004 Blue integumentary structural colours in dragonflies (Odonata) are not produced by incoherent Tyndall scattering. *J. Exp. Biol.* **207**, 3999–4009. (doi:10.1242/jeb.01240)

Prum, R. O., Quinn, T. & Torres, R. H. 2006 Anatomically diverse butterfly scales all produce structural colours by coherent scattering. *J. Exp. Biol.* **209**, 748–765. (doi:10.1242/jeb.02051)

Rutowski, R. L., Macedonia, J. M., Merry, J. W., Morehouse, N., Yturralde, K., Taylor-Taft, L., Gaalema, D., Kemp, D. J. & Papke, R. S. 2007 Iridescent ultraviolet signal in the orange sulphur butterfly (*Colias eurytheme*): spatial, temporal and spectral properties. *Biol. J. Linn. Soc.* **90**, 349–364. (doi:10.1111/j.1095-8312.2007.00749.x)

Schultz, T. D. & Rankin, M. A. 1985 Developmental changes in the interference reflectors and colorations of tiger beetles (*Cicindela*). *J. Exp. Biol.* **117**, 111–117.

Shawkey, M. D., Morehouse, N. I. & Vukusic, P. 2009 A protean palette: colour materials and mixing in birds and butterflies. *J. R. Soc. Interface* **6**, S221–S231. (doi:10.1098/rsif.2008.0459.focus)

Shimada, R. & Kawaguchi, Y. 2005 Spectral BRDF creation for structural colors. In *ACM Intern. Conf. Proc. Ser.*, vol. 157, pp. 16–21. See http://portal.acm.org/citation.cfm?id=1187009.

Silberglied, R. & Taylor, O. R. 1973 Ultraviolet differences between the sulphur butterflies, *Colias eurytheme* and *C. philodice*, and a possible isolating mechanism. *Nature* **241**, 406–408. (doi:10.1038/241406a0)

Smentkowski, V., Ostrowski, S., Olson, E., Cournoyer, J., Dovidenko, K. & Potyrailo, R. 2006 Exploration of a butterfly wing using a diverse suite of characterization techniques. *Microsc. Microanal.* **12**(Suppl. 2), 1228. (doi:10.1017/S1431927606067845)

Stavenga, D. G. 2002 Reflections on colourful butterfly eyes. *J. Exp. Biol.* **205**, 1077–1085.

Stavenga, D. G., Stowe, S., Siebke, K., Zeil, J. & Arikawa, K. 2004 Butterfly wing colours: scale beads make white pierid wings brighter. *Proc. R. Soc. B* **271**, 1577–1584. (doi:10.1098/rspb.2004.2781)

Stavenga, D. G., Giraldo, M. A. & Hoenders, B. J. 2006*a* Reflectance and transmittance of light scattering scales stacked on the wings of pierid butterflies. *Opt. Express* **14**, 4880–4890. (doi:10.1364/OE.14.004880)

Stavenga, D. G., Foletti, S., Palasantzas, G. & Arikawa, K. 2006*b* Light on the moth-eye corneal nipple array of butterflies. *Proc. R. Soc. B* **273**, 661–667. (doi:10.1098/rspb.2005.3369)

Stavenga, D. G., Leertouwer, H. L., Pirih, P. & Wehling, M. F. 2009 Imaging scatterometry of butterfly wing scales. *Opt. Express* **17**, 193–202. (doi:10.1364/OE.17.000193)

Sweeney, A., Jiggins, C. & Johnsen, S. 2003 Polarized light as a butterfly mating signal. *Nature* **423**, 31–32. (doi:10.1038/423031a)

Taflove, A. & Hagness, S. C. 2005 *Computational electrodynamics: the finite-difference time-domain method*, 3rd edn. Boston, MA: Artech House.

Vigneron, J. P., Rassart, M., Vandenbem, C., Lousse, V., Deparis, O., Biró, L. P., Dedouaire, D., Cornet, A. & Defrance, P. 2006 Spectral filtering of visible light by the cuticle of metallic woodboring beetles and microfabrication of a matching bioinspired material. *Phys. Rev. E* **73**, 041 905. (doi:10.1103/PhysRevE.73.041905)

Vukusic, P. & Sambles, J. R. 2001 Shedding light on butterfly wings. *Proc. SPIE* **4438**, 85–95. (doi:10.1117/12.451481)

Vukusic, P. & Sambles, J. R. 2003 Photonic structures in biology. *Nature* **424**, 852–855. (doi:10.1038/nature01941)

Vukusic, P., Sambles, J. R., Lawrence, C. R. & Wootton, R. J. 1999 Quantified interference and diffraction in single *Morpho* butterfly scales. *Proc. R. Soc. B* **266**, 1403–1411. (doi:10.1098/rspb.1999.0794)

Vukusic, P., Sambles, J. R., Lawrence, C. R. & Wakely, G. 2000 Sculpted-multilayer optical effects in two species of *Papilio* butterfly. *Appl. Opt.* **40**, 1117–1125. (doi:10.1364/AO.40.001116)

Vukusic, P., Sambles, J. R., Lawrence, C. R. & Wootton, R. J. 2001 Structural colour—now you see it now you don't. *Nature* **410**, 36. (doi:10.1038/35065161)

Vukusic, P., Wootton, R. J. & Sambles, J. R. 2004 Remarkable iridescence in the hindwings of the damselfly *Neurobasis chinensis chinensis* (Linnaeus) (Zygoptera: Calopterygidae). *Proc. R. Soc. B* **271**, 595–601. (doi:10.1098/rspb.2003.2595)

Vukusic, P., Kelly, R. & Hooper, I. 2009 A biological sub-micron thickness optical broadband reflector characterised using both light and microwaves. *J. R. Soc. Interface* **6**, S193–S201. (doi:10.1098/rsif.2008.0345.focus)

Welch, V. L. 2005 Photonic crystals in biology. In *Structural colors in biological systems—principles and applications* (eds S. Kinoshita & S. Yoshioka), pp. 53–71. Osaka, Japan: Osaka University Press.

Welch, V., Lousse, V., Deparis, O., Parker, A. & Vigneron, J. P. 2007 Orange reflection from a three-dimensional photonic crystal in the scales of the weevil *Pachyrrhynchus congestus pavonius* (Curculionidae). *Phys. Rev. E* **75**, 1–9. (doi:10.1103/PhysRevE.75.041919)

Wilts, B. D., Leertouwer, H. L. & Stavenga, D. G. 2009 Imaging scatterometry and microspectrophotometry of lycaenid butterfly wing scales with perforated multilayers. *J. R. Soc. Interface* **6**, S185–S192. (doi:10.1098/rsif.2008.0299.focus)

Wright, W. D. 1963 The rays are not coloured. *Nature* **198**, 1239–1244. (doi:10.1038/1981239a0)

Yeh, P. 2005 *Optical waves in layered media*. Hoboken, NJ: Wiley-Interscience.

Yoshioka, S. & Kinoshita, S. 2002 Effect of macroscopic structure in iridescent color of the peacock feathers. *Forma* **17**, 169–181.

Yoshioka, S. & Kinoshita, S. 2006*a* Single-scale spectroscopy of structurally colored butterflies: measurements of quantified reflectance and transmittance. *J. Opt. Soc. Am. A* **23**, 134–141. (doi:10.1364/JOSAA.23.000134)

Yoshioka, S. & Kinoshita, S. 2006*b* Structural or pigmentary? Origin of the distinctive white stripe on the blue wing of a *Morpho* butterfly. *Proc. R. Soc. B* **273**, 129–134. (doi:10.1098/rspb.2005.3314)

Yoshioka, S. & Kinoshita, S. 2007 Polarization-sensitive color mixing in the wing of the Madagascan sunset moth. *Opt. Express* **15**, 2691–2701. (doi:10.1364/OE.15.002691)

Yoshioka, S., Nakamura, E. & Kinoshita, S. 2007 Origin of two-color iridescence in rock dove's feather. *J. Phys. Soc. Jpn* **76**, 013 801. (doi:10.1143/JPSJ.76.013801)

Zi, J., Yu, X., Li, Y., Hu, X., Xu, C., Wang, X., Liu, X. & Fu, R. 2003 Coloration strategies in peacock feathers. *Proc. Natl Acad. Sci. USA* **100**, 12 576–12 578. (doi:10.1073/pnas.2133313100)